

## Triblock Colloids for Directed Self-Assembly

Qian Chen,<sup>†</sup> Erich Diesel,<sup>†</sup> Jonathan K. Whitmer,<sup>‡</sup> Sung Chul Bae,<sup>†</sup> Erik Luijten,<sup>§,||</sup> and Steve Granick<sup>\*,†,‡,⊥</sup>

<sup>†</sup>Department of Materials Science and Engineering, <sup>‡</sup>Department of Physics, and <sup>⊥</sup>Department of Chemistry, University of Illinois, Urbana, Illinois 61801, United States

<sup>§</sup>Department of Materials Science and Engineering and <sup>||</sup>Department of Engineering Sciences and Applied Mathematics, Northwestern University, Evanston, Illinois 60208, United States

**S** Supporting Information

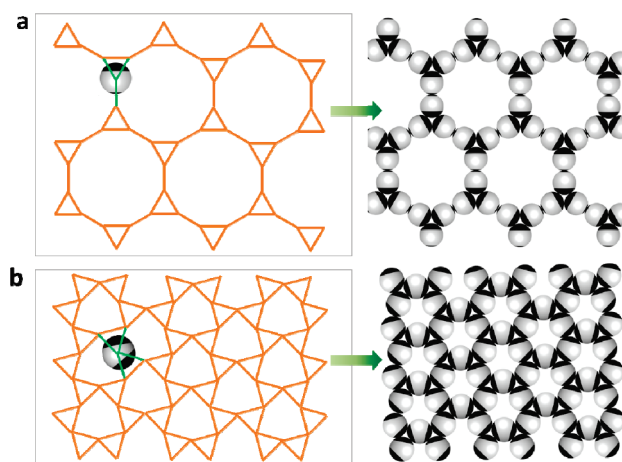
**ABSTRACT:** Methods for functionalizing micrometer-sized colloidal spheres with three or more zones of chemical functionality (ABA or ABC) are described. To produce ABA triblock colloids, we functionalized the north pole, south pole, and equator to produce what we call X, Y, and K functionality according to the number of allowed nearest neighbors and their spatial arrangements. These synthesis methods allowed targeting of various lattice structures whose bonding between neighboring particles in liquid suspension was visualized in situ by optical microscopy.

A core question in materials science is how to encode non-trivial organized structures within simple building blocks. Solving this problem is subject to various conditions. First, the building blocks should be sufficiently simple to allow facile synthesis or fabrication; second, building blocks with different topological design and surface interactions should be within reach in order to access a variety of targeted organized structures. Here we are concerned with planar arrangements. The potential relevance ranges from seeking laboratory methods to tile space with colloids in specific geometric patterns,<sup>1a</sup> which sometimes might possess specific mechanical properties,<sup>1b,c</sup> to designing selective membranes and host platforms.<sup>2</sup> A recent report from this laboratory described methods for functionalizing latex spheres to make them hydrophobic at their poles, leading to the directed self-assembly of a kagome lattice pattern in which each sphere was coordinated with four neighbors, two at each pole.<sup>2b</sup> However, only one single structure of self-assembly significance was demonstrated, as systematically tuning the sizes and positions of the irregular patch shapes was challenging in that study.

Here we introduce the concept that varying the area of surface functionalization serves to modify the valence (i.e., potential coordination with neighbors) as well as the topological arrangement of areas on neighboring particles that are functionalized either to attract or to repel. This communication describes robust fabrication methods for producing the needed particles.

Consider panels a and b of Scheme 1. These concern cases of arrangements of monodisperse spheres; their mixtures present an obvious generalization. The connections between points on a planar lattice then have equal length. The “X” bonding geometry (two nearest neighbors on each pole) was introduced previously.<sup>2b</sup> If a given colloid possesses room to attract one neighbor at one end and two neighbors at the opposite end, this

### Scheme 1. Design of Triblock Spheres for Directed Self-Assembly of Open Colloidal Networks<sup>a</sup>



<sup>a</sup> (a) Triblock spheres with a “Y” bonding motif can produce a truncated hexagonal lattice with one nearest neighbor at one pole and two nearest neighbors at the opposite pole of the sphere. (b) Triblock spheres with a “K” bonding motif can produce a distorted kagome lattice that is predicted to differ from the standard kagome lattice with respect to its mechanical properties.<sup>1c</sup>

leads to a building block with a “Y”-shaped interaction pattern. Such a pattern might be implemented by functionalizing spheres with a small patch on one end and a patch large enough to hold two adjacent neighbors on the other. Scheme 1a shows that this can generate truncated hexagonal patterns.<sup>1</sup> Scheme 1b shows that following the same logic, a deliberately distorted kagome lattice<sup>1c</sup> can be created from building blocks with a “K”-shaped bonding geometry, which could be realized by functionalizing spheres with two patches that are sufficiently large to accommodate two neighbors each but whose center-to-center axis does not pass through the center of the sphere. Pursuing this concept on the experimental side, we chose to implement the building blocks of both of these lattices (i.e., control of patch size for Y-shaped interactions and control of patch topology for K-shaped interactions) as well as other possibilities outlined below. In the discussion presented here, we emphasize the synthetic aspects.

Received: March 15, 2011

Published: April 25, 2011

From among the synthetic strategies previously known to produce triblock spheres,<sup>2b,3</sup> including elastomeric stamping one pole at a time,<sup>2b,3a–3c</sup> earlier work by this laboratory was predicated on glancing-angle deposition of gold coatings followed by thiol surface functionalization.<sup>2b</sup> Despite the usefulness of this method,<sup>2b</sup> the shape and size of coatings formed by glancing-angle deposition suffer from shadowing by neighboring particles during metal deposition, unless the requirement of a strictly close-packed monolayer of parent particles is met.<sup>3c</sup> The resulting irregular shapes of the gold patches can complicate the interactions with other particles during subsequent self-assembly.<sup>2b,3c</sup> The methods described here create uniform triblock spheres with patches shaped as spherical caps whose sizes and mutual positions can be tuned.

Particles spread onto a flat substrate are first coated from above on one hemisphere, flipped over via contact stamping [Figure 1a; also see the Supporting Information (SI)], and then

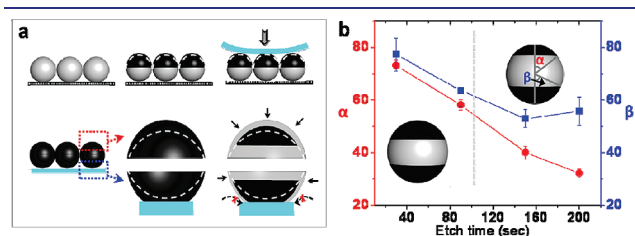


**Figure 1.** Synthesis of triblock spheres. (a) Parent colloidal spheres on a flat substrate are first coated on one hemisphere with 2 nm Ti and 25 nm Au (black), then pressed against a sticky PDMS stamp to release the uncoated hemisphere, flipped over, and decorated with the same coating again. The stamp is subsequently immersed in a gold-etching solution. The gold coatings on the top and bottom shrink differently. (b) The angles  $\alpha$  and  $\beta$  (defined in the inset) are a measure of the size of the top (red circles) and bottom (blue squares) gold patches, respectively. Plotted against etch time, they illustrate how these patches etch at different rates.

coated from above on the other, newly exposed hemisphere. During metal deposition, any monolayer arrangement of the particles from loosely packed to crystalline is permitted, since there is no possibility of shadowing. Notably, coating from above produces the thickest coating at the poles, with the thickness progressively tapering off toward the equator (see Supporting Figure 1 and Supporting Discussions in the SI). Subsequent etching causes these radially symmetric caps of nonuniform thickness to gradually decrease in size. Implementing this idea with polydimethylsiloxane (PDMS) stamps, we immerse particle layers, while they sit on the PDMS stamp, into a gold-etching solution.<sup>4</sup> The etching proceeds at a uniform rate with removal of the thinnest coatings first, causing the hemispheres to shrink controllably and uniformly from the edge, producing spherical caps. This process generates functionalized spheres with high monodispersity. The experience of this laboratory is that monodisperse building blocks are crucial for their subsequent assembly with high fidelity into targeted structures.

The conformal PDMS stamp protects occluded regions during the chemical etching. We have found that regardless of etching time, areas in contact with the stamp remain intact. Such a difference in etching microenvironments (Figure 1a) for the upper and lower patches can be significant. The top and bottom halves initially are etched at the same rate, but then the upper patch continues to shrink whereas the lower patch touching the stamp retains a size comparable with the contact area (Figure 1b). Thus, triblock spheres with either an X- or Y-shaped bonding geometry can be harvested from a single batch, by quenching the etching after different elapsed times. Figure 2a,b illustrates this for 2  $\mu\text{m}$  silica spheres, where the patches can be discerned in the scanning electron microscopy (SEM) images because of the stronger scattering from the conductive gold surface. In this experiment, the second gold deposition was perpendicular to the PDMS stamp. In addition to its control by etching, the size of the larger cap (i.e., the lower patch) can be tuned by controlling the softness of the elastomer stamp.<sup>3a</sup>

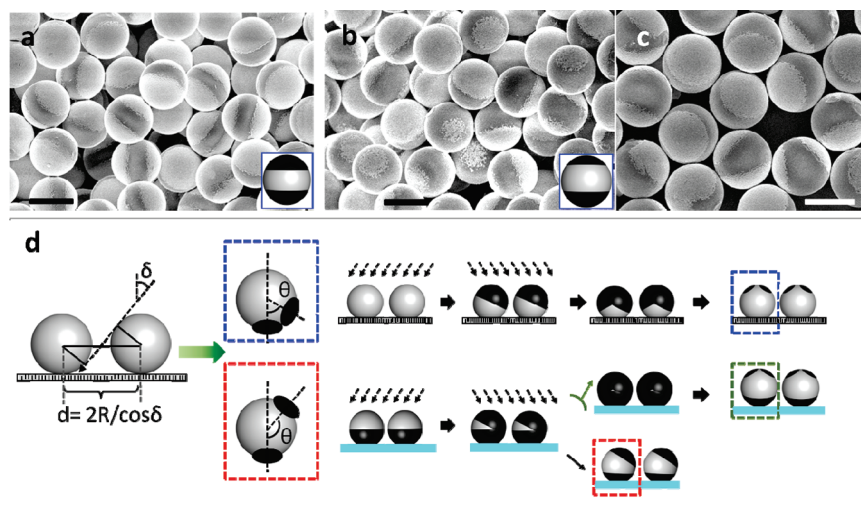


**Figure 2.** Examples of as-synthesized triblock spheres. (a–c) SEM images of particles with (a) X-shaped and (b) Y-shaped surface functionalization generated by ending the etching process at different stages as well as (c) K-shaped surface functionalization generated by tilting the second deposition beam  $30^\circ$  with respect to the normal direction of the particle layer. (d) Schematic diagrams of how, in principle, multiple tilted depositions from different angles can produce multiblock particles. This requires that the particles be spaced sufficiently far apart to avoid shadowing (i.e., at a minimum separation  $d = 2R/\cos \delta$  for a beam angle  $\delta$  and particle radius  $R$ ). Sequential deposition onto the same pole from different directions can produce triblock spheres with patches arranged at  $\theta < 90^\circ$ , as highlighted in the blue dashed box. The case of  $\theta > 90^\circ$ , highlighted in the red dashed box, can be combined with extra coatings on the upper pole to produce multiblock spheres (green dashed box). In panels (a–c), the scale bars represent 2  $\mu\text{m}$ .

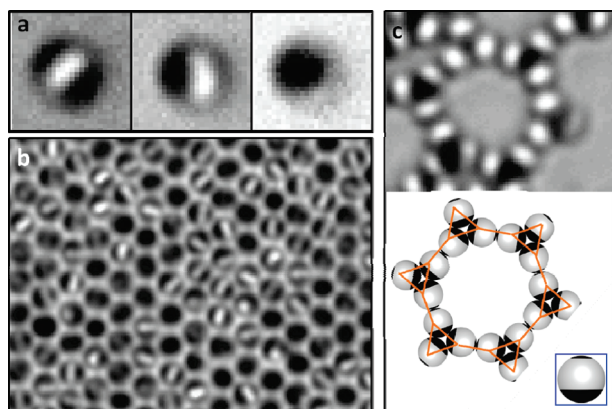


**Figure 3.** Triblock spheres visualized by bright-field optical microscopy. (a) Images of an individual sphere with X-shaped surface functionalization. Metal patches appear black and silica patches appear white, showing the particle orientation. (b) Example of a hexagonal lattice formed by these symmetric triblock, X-type silica spheres in deionized water, the poles being hydrophobic and the middle band charged. (c) Example of the dodecagonal pore of a truncated hexagonal lattice formed from triblock silica spheres with Y-shaped bonding geometry, where the gold patches were rendered hydrophobic via thiol chemistry.

It is also possible to tilt the beam in the second deposition to control the relative orientation of the two patches. The only requirement is that the particles are sufficiently separated on the planar substrate to prevent shadowing by their neighbors. Combined with proper etching time, this gives the K-shaped bonding geometry shown in Figure 2c. With this approach, patches can be oriented at almost any angle from opposite poles of the sphere to close together near the same pole (Figure 2d), the latter being accomplished by using two tilted depositions from different directions. We envision that this strategy can be generalized by a sequence of additional coatings to produce more complex coating geometries with an arbitrarily large number of patches, such as the example of spheres with three patches shown in Figure 2d.

It is easy to visualize the resulting particles by optical microscopy because even very thin gold patches provide the needed optical contrast to silica (Figure 3a); it should be noted that the metal coating appears black in these images, showing how the particles are oriented. Images of a collection of particles (Figure 3b) show how monodisperse the particles are. Although this communication focuses on synthesis rather than targeted assembly, we emphasize that optical visualization also can show how particles are oriented after they assemble and thus reveal the bonding network of the self-assembled structure. For example, Figure 3c shows a dodecagonal pore formed by the Y-shaped triblock spheres; here the silica rims are white and the gold rims black. The gold patches were rendered hydrophobic using thiol chemistry, and the pores self-assembled after triblock spheres in aqueous suspension sedimented to the bottom of the sample cell. We anticipate that with image analysis, both the temporal and spatial distribution of particle orientations can be quantified. This could provide, for example, insight into the vibrational modes of this and other complex structures.<sup>1c,5</sup>

The synthetic method and particle design strategy described herein enable a variety of applications in targeted self-assembly. Although it has been illustrated here for the surface-chemical modification of silica spheres with gold coatings, in principle the

method could be generalized to other techniques of surface functionalization,<sup>6</sup> different material coatings,<sup>6,7</sup> and surface functionalization of particles with more complex shapes. Shadowing can be avoided in the case of spheres by not packing the particles too closely, and methods to achieve this are known.<sup>8</sup> For more complex shapes, use of atomic layer deposition would further generalize the approach.

## ■ ASSOCIATED CONTENT

**S Supporting Information.** Experimental procedures and additional discussions. This material is available free of charge via the Internet at <http://pubs.acs.org>.

## ■ AUTHOR INFORMATION

### Corresponding Author

sgranick@illinois.edu

## ■ ACKNOWLEDGMENT

This work was supported at the University of Illinois by the U.S. Department of Energy, Division of Materials Science, under Award DE-FG02-07ER46471 through the Frederick Seitz Materials Research Laboratory at the University of Illinois at Urbana–Champaign. E.D. acknowledges NSF Grant CBET-0853737. J.K.W. and E.L. acknowledge NSF Grants DMR-0346914 and DMR-1006430.

## ■ REFERENCES

- (1) (a) Grünbaum, B.; Shephard, G. C. *Tilings and Patterns*; Freeman: New York, 1987. (b) Ueda, K.; Dotera, T.; Gemma, T. *Phys. Rev. B* **2007**, *75*, No. 195122. (c) Kapko, V.; Treacy, M. M. J.; Thorpe, M. F.; Guest, S. D. *Proc. R. Soc. London, Ser. A* **2009**, *465*, 3517.
- (2) (a) Doppelbauer, G.; Bianchi, E.; Kahl, G. *J. Phys.: Condens. Matter* **2010**, *22*, No. 104105. (b) Chen, Q.; Bae, S. C.; Granick, S. *Nature* **2011**, *469*, 381. (c) Romano, F.; Sciortino, F. *Nat. Mater.* **2011**, *10*, 171. (d) Russo, J.; Tavares, J. M.; Teixeira, P. I. C.; Telo da Gama, M. M.; Sciortino, F. *Phys. Rev. Lett.* **2011**, *106*, No. 085703.
- (3) (a) Jiang, S.; Granick, S. *Langmuir* **2009**, *25*, 8915. (b) Pawar, A. B.; Kretzschmar, I. *Langmuir* **2009**, *25*, 9057. (c) Kaufmann, T.; Gokmen, M. T.; Wendeln, C.; Schneiders, M.; Rinnen, S.; Arlinghaus, H. F.; Bon, S. A. F.; Du Prez, F. E.; Ravoo, B. J. *Adv. Mater.* **2011**, *23*, 79. (d) Roh, K. H.; Martin, D. C.; Lahann, J. *J. Am. Chem. Soc.* **2006**, *128*, 6796.
- (4) (a) Xia, Y.; Zhao, X.-M.; Kim, E.; Whitesides, G. M. *Chem. Mater.* **1995**, *7*, 2332. (b) Bao, Z.; Chen, L.; Weldon, M.; Chandross, E.; Cherniavskaya, O.; Dai, Y.; Tok, J. B.-H. *Chem. Mater.* **2002**, *14*, 24.
- (5) Kaya, D.; Green, N. L.; Maloney, C. E.; Islam, M. F. *Science* **2010**, *329*, 656.
- (6) Love, J. C.; Estroff, L. A.; Kriebel, J. K.; Nuzzo, R. G.; Whitesides, G. M. *Chem. Rev.* **2005**, *105*, 1103.
- (7) Bauer, L. A.; Reich, D. H.; Meyer, G. J. *Langmuir* **2003**, *19*, 7043.
- (8) (a) Jiang, P.; McFarland, M. J. *J. Am. Chem. Soc.* **2005**, *127*, 3710. (b) Yan, X.; Yao, J.; Lu, G.; Zhang, J.; Yang, B. *J. Am. Chem. Soc.* **2005**, *127*, 7688. (c) Xia, Y.; Yin, Y.; Lu, Y.; McLellan, J. *Adv. Funct. Mater.* **2003**, *13*, 907.